OPEN ACCESS

Applied Physics Express 12, 012008 (2019) LETTER

https://doi.org/10.7567/1882-0786/aaf788

Influence of light absorption on the performance characteristics of UV LEDs with emission between 239 and 217 nm

Frank Mehnke*, Luca Sulmoni, Martin Guttmann, Tim Wernicke, and Michael Kneissl

Technische Universität Berlin, Institut für Festkörperphysik, Hardenbergstr. 36, EW 6-1, 10623 Berlin, Germany

*E-mail: mehnke@physik.tu-berlin.de

Received November 2, 2018; accepted December 10, 2018; published online January 4, 2019

The development of ultraviolet AlGaN multiple quantum well (MQW) light emitting diodes (LEDs) in the wavelength range between 239 and 217 nm is presented. The effects of aluminum composition in the MQW active region and of the underlying $Al_xGa_{1-x}N$:Si current spreading layer on the emission characteristics and operating voltages are investigated. A strong reduction in output power is observed with decreasing emission wavelength which is partly attributed to light absorption within the underlying $Al_xGa_{1-x}N$:Si. Additionally, a reduced carrier injection efficiency is identified as the root cause for the reduced emission power with decreasing emission wavelength. Emission powers at a dc current of 20 mA between 310 and 0.15 μW have been achieved for LEDs emitting between 239 and 217 nm. The maximum light output in pulsed mode operation of these LEDs ranged between 4.6 mW and 3.6 μW, respectively. © 2019 The Japan Society of Applied Physics

The demand for deep ultraviolet (UV) light emitting diodes (LEDs) is growing rapidly due to new applications in the area of gas sensing and medical diagnostics. For example, in the UV spectral region below 240 nm, applications such as gas sensing (NO: $\lambda = 226$ nm, NH_3: $\lambda = 217$ nm)[1,2] would greatly benefit from the development of LEDs with sufficiently high spectral power. However, the fabrication of such short wavelength AlGaN-based LEDs is very demanding as carrier injection and confinement as well as light extraction become extremely challenging.[3] In addition, the sheet and contact resistivities in n- and p-AlGaN layers as well as at the semiconductor/metal interfaces increase significantly with increasing aluminum mole fraction.[4,5] So far, the shortest wavelength AlN-based LED has been reported by Ref. 6 emitting at 210 nm with an optical output power (P_{opt}) of 0.125 μW and an external quantum efficiency (EQE) of 10^{-4}%. Reference 7 reported 222 and 227 nm LEDs operating in pulsed mode with $P_{opt} = 15$ μW and $P_{opt} = 150$ μW, respectively, corresponding to a maximum EQE of 0.003% and 0.2%. Recently, Refs. 8, 9 demonstrated cw operation of 226 nm and 229 nm LEDs utilizing p-type Si nanomembranes with $P_{opt} = 225$ μW and $P_{opt} = 160$ μW corresponding to EQEs of 0.2% and 0.03%, respectively. Furthermore, Ref. 10 presented 230 nm LEDs on bulk AlN exhibiting $P_{opt} = 210$ μW and an EQE of 0.025%. Recently, we demonstrated 263 nm to 235 nm LEDs exhibiting output powers between 880 μW for 263 nm and 2.1 μW for 235 nm emission corresponding to EQEs ranging from 0.933% to 0.002%, respectively.[11] After further optimization of the AlGaN heterostructure design, doping profile, and the AlGaN barrier composition, flip-chip mounted 232 nm LEDs were successfully deployed in a NO gas detection system.[2]

However, the root causes for the rapidly dropping emission power levels and EQEs with decreasing emission wavelength have not been well understood. Typically, this behavior is attributed to several mechanisms, mainly a reduced internal quantum efficiency (IQE), a reduced carrier injection efficiency (CIE), and a reduced light extraction efficiency (LEE)[10,11] due to the change of the optical polarization of the emitted light from transverse electric (TE) to transverse magnetic (TM) at emission wavelengths of around 240 nm[12,13] for fully strained multiple quantum wells (MQWs) on AlN. Besides these mechanisms, reabsorption of the emitted light within the n-side of the LED heterostructure is typically not considered. However, as the n-side conductivity strongly decreases with increasing aluminum mole fraction, there is a conductivity-transparency dilemma. In this paper, we have made a comprehensive study of the influence of the composition of the underlying $Al_xGa_{1-x}N$:Si current spreading layer on the emission characteristics and operation voltages of UV LEDs emitting between 239 and 217 nm. In particular, a variation of the aluminum composition of the AlGaN MQWs of LEDs grown on $Al_xGa_{1-x}N$:Si current spreading layer with aluminum mole fractions as high as $x = 0.95$ will be presented.

All LEDs have been grown by metalorganic vapor phase epitaxy on (0001) epitaxially laterally overgrown (ELO) AlN/sapphire[14] with threading dislocation densities (TDD) of 1×10^9 cm^{-2}.[15] After growth of an AlN buffer layer, a 1.2 μm thick Si-doped $Al_xGa_{1-x}N$ current spreading layer with $0.79 < x < 0.95$ was deposited. The composition of each layer was determined by X-ray diffraction with $\Delta x = 0.01$.[16] In order to reduce the resistivity of the current spreading layer, the silicon doping concentration was optimized by a variation of the SiH_4/III partial pressure ratio from 8×10^{-5} to 4×10^{-5} for different aluminum compositions.[5] The resulting Si-concentration as determined by wavelength dispersive X-ray spectroscopy ranged between 1.4×10^{19} cm^{-3} for $x = 0.79$ and 8×10^{18} cm^{-3} for $x = 0.95$.[16] Subsequently, a threefold $Al_xGa_{1-x}N/Al_yGa_{1-y}N$ MQW was deposited with an aluminum mole fraction of $0.68 < x < 0.86$ in the QWs and $0.80 < y < 0.97$ in the barriers. The QW and barrier thicknesses were kept constant at 1 nm and 5 nm, respectively. The heterostructure is completed by a 6 nm AlN electron blocking layer (EBL), a 25 nm thick Mg-doped $Al_{0.80}Ga_{0.20}N/Al_{0.70}Ga_{0.30}N$ short period superlattice hole injection layer, a 100 nm thick Mg-doped $Al_{0.37}Ga_{0.63}N/Al_{0.20}Ga_{0.80}N$ superlattice, and a 40 nm thick GaN:Mg contact layer. Note that the LEDs are designed as bottom emitters as the p-layers are non-transparent for the emitted light. After activation of the Mg-dopants, the heterostructures have been fabricated into UV LEDs with emitting areas ranging between 0.04 and 0.1 mm^2. V-based and

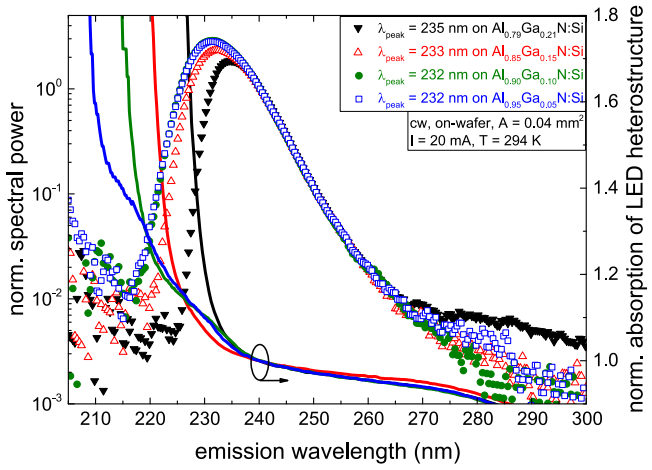

Fig. 1. (Color online) Representative 232 nm LED emission spectra (normalized at 240 nm) grown on $Al_xGa_{1-x}N$:Si with $x = 0.79$ (black triangles), $x = 0.85$ (open red triangles), $x = 0.90$ (green circles), $x = 0.95$ (open blue squares) as well as corresponding absorption measurements (also normalized at 240 nm) of the full LED heterostructures (solid lines).

Pd-based electrodes were used as n- and p-contacts, respectively. After processing, the LEDs were measured on-wafer without any active cooling by electroluminescence spectroscopy (EL) using a calibrated compact optical fiber spectrometer and a calibrated UV enhanced Si-photodiode. The luminescence contributions of the AlGaN MQWs were separated by fitting a Gaussian function. In cw operation, nine LEDs have been measured across each wafer in order to check for wafer homogeneity and the averaged emission powers and operation voltages are given in the paper. For pulsed mode EL measurements, a dc bias voltage close to the turn-on voltage was applied via a bias tee and current pulses with a pulse width of 1 μs and a repetition rate of 20 kHz were applied. Transmission measurements were performed on $Al_xGa_{1-x}N$:Si calibration samples with backside polished sapphire substrates and full LED heterostructures without backside polishing using a Shimadzu UV-2600 UV-VIS spectrophotometer. The relative absorption $\alpha \cdot d$ was calculated using Beer–Lambert law.

In order to maximize the wall plug efficiency (WPE) of deep UV LEDs, a tradeoff between the absorption and the conductivity of the $Al_xGa_{1-x}N$:Si current spreading layer has to be found. The UV absorption can be reduced by increasing the aluminum content of the $Al_xGa_{1-x}N$:Si current spreading layer, e.g. $Al_{0.80}Ga_{0.20}N$:Si with a bandgap of $E_{Gap} \approx 5.39$ eV is transparent to emission wavelength as short as 232 nm. However, inhomogeneous broadening of the UV LED emission spectrum and sub-bandgap absorption of the AlGaN:Si current spreading layer can lead to partial absorption of the short wavelength contributions of the UV LED emission spectrum. In order to investigate this, 232 nm LEDs have been grown on $Al_xGa_{1-x}N$:Si current spreading layers with aluminum composition ranging between $x = 0.79$ and $x = 0.95$. Figure 1 shows representative emission spectra of 232 nm LEDs at a fixed dc current of 20 mA grown on $Al_xGa_{1-x}N$:Si with $x = 0.79$ (black triangles), $x = 0.85$ (open red triangles), $x = 0.90$ (green circles), and $x = 0.95$ (open blue squares) as well as the corresponding absorption spectra (solid lines) measured on the full LED heterostructures (absorption in the AlGaN:Mg superlattice and GaN:Mg is similar for all LEDs and not shown). The spectra were normalized at 240 nm assuming negligible absorption for all $Al_xGa_{1-x}N$:Si current spreading layers at this wavelength. The spectral power of the long wavelength contributions (i.e. at wavelengths above peak emission) is very similar for all LEDs. This indicates that the inhomogeneous broadening of the emission spectra is independent of the aluminum composition of the underlying $Al_xGa_{1-x}N$:Si. In contrast, on the short wavelength side of the emission spectrum (i.e. at wavelengths below peak emission), a strong reduction in spectral power is observable for the LEDs grown on $Al_{0.85}Ga_{0.15}N$:Si and $Al_{0.79}Ga_{0.21}N$:Si. The cutoff of the short wavelength contributions of the LED spectra (i.e. the wavelength at which the spectral power falls below 10% of the normalized value) is shifted from 228 nm for growth on $Al_{0.79}Ga_{0.21}N$:Si to 224 nm for growth on $Al_{0.85}Ga_{0.15}N$:Si. For LEDs grown on $Al_{0.90}Ga_{0.10}N$:Si and $Al_{0.95}Ga_{0.05}N$:Si, the spectra are identical indicating full transparency of the current spreading layers. Additionally, a shift in the peak emission wavelength is observed with decreasing aluminum composition of the $Al_xGa_{1-x}N$:Si current spreading layer from 232 nm for $x = 0.95$ and $x = 0.90$ to 233 nm for $x = 0.85$ and to 235 nm for $x = 0.79$. This is accompanied by a slight reduction in spectral power at peak emission due to sub-bandgap absorption. Consequently, one would prefer high aluminum mole fraction AlGaN:Si current spreading layers in order to avoid the reabsorption of the emitted light. Unfortunately, increasing the aluminum content in the $Al_xGa_{1-x}N$:Si current spreading layer induces an exponential increase of the layer resistivity.[5] Furthermore, the formation of n-contacts on $Al_xGa_{1-x}N$:Si layers with high aluminum content becomes more challenging[4] which originates in the decreasing electron affinity of $Al_xGa_{1-x}N$ with increasing aluminum mole fraction.[17] Additionally, difficulties of Si-doping of $Al_xGa_{1-x}N$ with aluminum compositions $x > 0.80$[5] limits the ionized donor concentration and results in relatively high contact resistivities with non-ohmic behavior.

To improve the n-contacts on $Al_xGa_{1-x}N$:Si, the V/Al/Ni/Au electrode configuration and the rapid thermal annealing during contact formation (800 °C for 60 s under N_2 atmosphere, details will be published elsewhere) was optimized. The n-contact resistivities evaluated by linear transfer length method (TLM) at 100 Acm^{-2} were as low as 2.5×10^{-3} Ωcm^2 for $x = 0.79$, 2.8×10^{-3} Ωcm^2 for $x = 0.85$, 3.5×10^{-3} Ωcm^2 for $x = 0.90$, and 7.6×10^{-3} Ωcm^2 for $x = 0.95$. The applied bias voltage at a fixed current of 1 mA for a contact spacing of 8 μm increases from 0.24 V for contacts on $Al_xGa_{1-x}N$:Si with $x = 0.79$ to 1.1 V for $x = 0.85$ to 1.9 V for $x = 0.90$ to 5.4 V for $x = 0.95$. Both the contact resistivity and the voltage at 1 mA gradually increase with the aluminum composition. This is also observable in the *IV* characteristics of the LEDs as the forward voltages at 20 mA increase from 7 V to 7.9 V, 10.2 V, and 17.3 V for $Al_xGa_{1-x}N$:Si layers with $x = 0.79$, $x = 0.85$, $x = 0.90$, and $x = 0.95$, respectively, showing the same trend as the TLM measurements. Since higher sheet and contact resistivities result in Joule heating (especially for dc operation at higher currents) which is detrimental for the EQE and WPE of the devices, the aluminum mole fraction of the $Al_xGa_{1-x}N$:Si current spreading layer needs to be chosen as low as possible, without reducing the spectral power at the application relevant wavelength.

In order to explore the limits for shorter wavelength LEDs, the composition of the $Al_xGa_{1-x}N/Al_yGa_{1-y}N$ MQW active

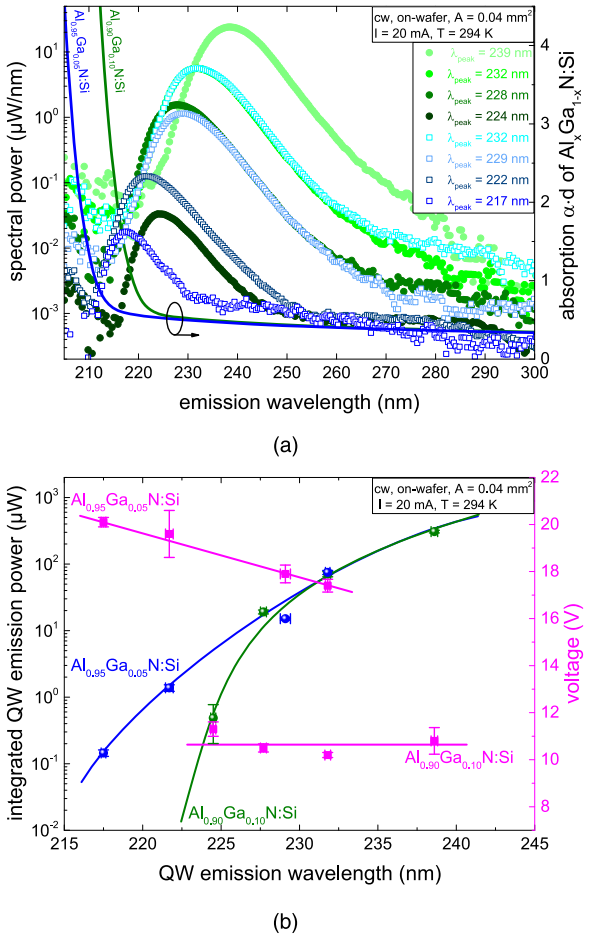

Fig. 2. (Color online) (a) Spectral power of representative LEDs with varied emission wavelength grown on $Al_xGa_{1-x}N$:Si with $x = 0.90$ (greenish circles) and $x = 0.95$ (open blueish squares) as well as absorption spectra of backside polished $Al_xGa_{1-x}N$:Si calibration samples with equal composition (solid lines). (b) Averaged integrated QW EL emission power including standard deviation of nine devices (green and blue for growth on $x = 0.90$ and $x = 0.95$) and operation voltage at 20 mA (magenta).

region was varied between $0.68 < x < 0.86$ and $0.80 < y < 0.97$, keeping the band offset between QWs and barriers constant. The $Al_xGa_{1-x}N$:Si current spreading layer compositions $x = 0.90$ and $x = 0.95$ were chosen in order to avoid light absorption for shorter wavelength LEDs. Representative EL emission spectra of the realized UV LEDs as well as absorption spectra of backside polished $Al_xGa_{1-x}N$:Si calibration samples are shown in Fig. 2(a). Here, green filled circles refer to spectra of LEDs grown on $Al_{0.90}Ga_{0.10}N$:Si and blue open circles refer to spectra of LEDs grown on $Al_{0.95}Ga_{0.05}N$:Si. In Fig. 2(b), the averaged QW EL emission power including the standard deviation (green and blue) and applied bias voltage (magenta) are plotted versus the peak emission wavelength ranging between 239 and 217 nm. The performances of all LEDs were evaluated at a dc current of 20 mA using a constant emitting area of 0.04 mm^2. All LEDs exhibit dominant QW emission but the peak spectral power is strongly reduced from 24 $\mu W\ nm^{-1}$ for emission at 239 nm to 18 $nW\ nm^{-1}$ for emission at 217 nm. The long wavelength contributions above 300 nm of all LEDs [not shown in Fig. 2(a)] are lower than 4 $nW\ nm^{-1}$. The corresponding averaged QW EL emission power are shown in Fig. 2(b). As indicated by the standard deviation, all investigated samples show only a small variation in emission wavelength and emission power over the wafer. The integrated QW emission power decreases more than three orders of magnitude with decreasing emission wavelength from 310 μW for 239 nm peak emission to 0.15 μW for 217 nm peak emission. The drop in the emission power is even more pronounced for LEDs on $Al_{0.90}Ga_{0.10}N$:Si current spreading layers, clearly visible for the 224 nm LED with an QW emission power of 0.49 μW in comparison to the 222 nm LED grown on $Al_{0.95}Ga_{0.05}N$:Si exhibiting 1.4 μW although having a shorter emission wavelength. The later observation can be attributed to absorption of the short wavelength contributions of the emission spectra as the absorption of the $Al_{0.90}Ga_{0.10}N$:Si layers already increases at around 225 nm as depicted in the absorption spectrum in Fig. 2(a). Also, for the 217 nm LED light absorption of the short wavelength contributions of the emission spectrum within the $Al_{0.95}Ga_{0.05}N$:Si current spreading layer may not be negligible as the absorption starts to increase at around 218 nm. Consistently with the LEDs grown on different $Al_xGa_{1-x}N$:Si current spreading layers with $0.79 < x < 0.95$, the operating voltages for the LEDs on $Al_{0.90}Ga_{0.10}N$:Si are between 10.2 and 11.3 V and significantly lower than the operating voltages for LEDs on $Al_{0.95}Ga_{0.05}N$:Si which range from 17.4 to 20.1 V. An increase in operation voltage with decreasing emission wavelength by 0.25 V is expected due to the larger bandgap. The stronger increase for the LEDs grown on $Al_{0.95}Ga_{0.05}N$:Si will be subject to further investigations. Regardless of any improvements in terms of EQE or QW emission power provided by an increased $Al_xGa_{1-x}N$:Si composition, a reduction in the WPE by factor of two has to be considered in the following. However, at shorter emission wavelengths for which the light absorption is relevant, i.e. below 228 nm for growth on $Al_{0.90}Ga_{0.10}N$:Si, growth on $Al_{0.95}Ga_{0.05}N$:Si is preferable as emission power, EQE, and WPE become superior for this current spreading layer compositions.

While absorption within the $Al_xGa_{1-x}N$:Si current spreading layer is one reason for the drastic decrease in emission power with decreasing emission wavelength, it cannot be the only explanation for the observed behavior. By taking into account the UV LED emission characteristics and the absorption spectra, the influence of absorption can be excluded for LEDs with emission wavelengths above 222 nm, 228 nm, 234 nm, and 240 nm for growth on $Al_xGa_{1-x}N$:Si with an aluminum composition $x = 0.95$, $x = 0.90$, $x = 0.85$, and $x = 0.80$, respectively. As light absorption can be excluded for these LEDs, the root causes for the observed decrease in emission power with decreasing emission wavelength (310 μW for 239 nm emission to 1.4 μW for 222 nm emission) must originate from a reduced IQE, LEE, and CIE. As all LEDs have been grown pseudomorphically on similar ELO AlN/sapphire, the TDD and therefore the IQE is expected to be the same for all samples.[18] Nevertheless, the IQE might also be affected at shorter wavelengths by an increase in point defect density in higher aluminum mole fraction alloys[19] when increasing the QW composition from $x = 0.68$ to $x = 0.82$. However, the absolute change in QW composition is rather small. Also, the band offsets between QWs and barriers and the polarization fields should be identical as the barrier composition was adjusted together with the QW composition. Therefore, the influence of a decreasing IQE with decreasing emission wavelength is unlikely to explain the reduction of the emission power by more than three orders of magnitude. The LEE is strongly affected by the

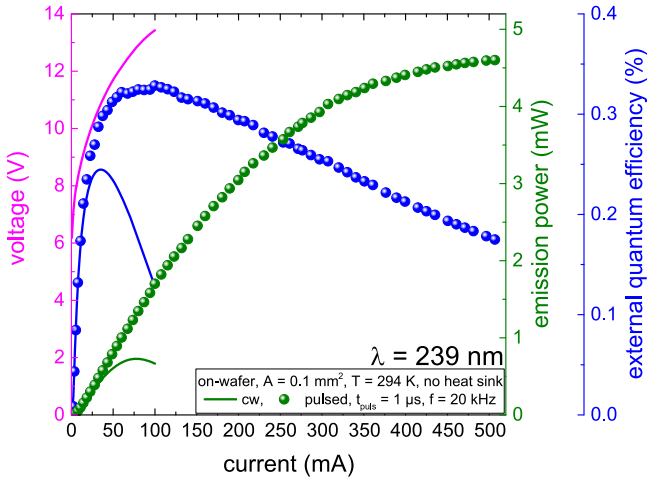

Fig. 3. (Color online) Operation voltage (magenta), emission power (green), and EQE (blue) of a 239 nm LED grown on $Al_{0.90}Ga_{0.10}N$:Si under cw (solid lines) and pulsed mode operation (bullets) measured on-wafer without active cooling.

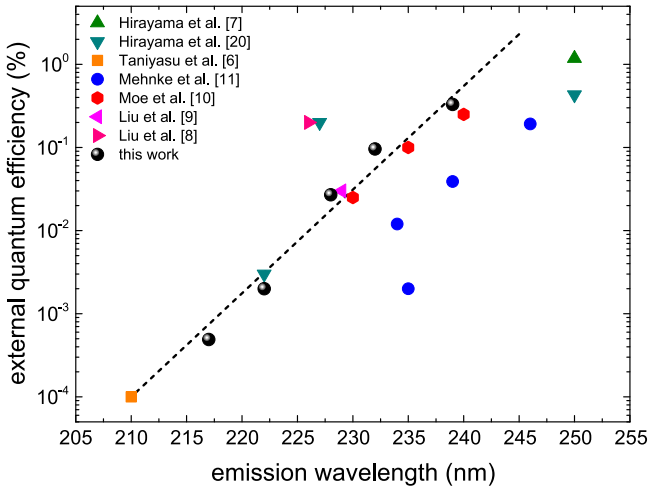

Fig. 4. (Color online) Maximum achieved EQEs in pulsed mode operation in dependence of the emission wavelength compared to recent literature.[6–11,20]

optical polarization of the emitted light. As previous studies have shown, the polarization of light emission from AlGaN QWs undergoes a transition from dominant TE to dominant TM at an emission wavelength of around 240 nm.[13] This is consistent with measurements of the degree of polarization $P = (I_{TE} - I_{TM})/(I_{TE} + I_{TM})$ of the investigated samples changing from unpolarized emission ($P = 0$) for the 239 nm LED to dominant TM polarized emission ($P = -0{,}7$) for the 222 nm LED. Nevertheless, ray tracing simulations of the LEE for different degree of polarization of light emission and taking into account an absorbing p-side, a rough sapphire backside, and scattering at the ELO pattern (details will be published elsewhere) reveal only a small reduction in the LEE from 2.9% for emission at 239 nm to 1.7% for emission at 222 nm. Hence, the root cause for the reduced emission power with decreasing emission wavelength most likely needs to be ascribed to a reduced CIE. As the composition of the QWs and barriers increases, the conduction band offset towards the AlN EBL drastically decreases.[11] This leads to increasing electron leakage into the p-side of the LED and recombination of charge carriers outside the active region thus not contributing to QW luminescence. The quantitative analysis of the CIE is quite challenging and will require further investigations.

Finally, in order to investigate the maximum device performance and EQE, a 239 nm, a 232 nm, and a 228 nm LED grown on $Al_{0.90}Ga_{0.10}N$:Si as well as a 222 nm and a 217 nm LED grown on $Al_{0.95}Ga_{0.05}N$:Si have been measured in pulsed mode operation. The emitting area for the LEDs on $Al_{0.90}Ga_{0.10}N$:Si was 0.1 mm^2 whereas the emitting area for the LEDs on $Al_{0.95}Ga_{0.05}N$:Si was 0.04 mm^2 in order to take into account the reduced current spreading length in these higher resistive layers. Exemplary, Fig. 3 shows the LIV characteristics of the 239 nm LED grown on $Al_{0.90}Ga_{0.10}N$:Si. The emission power maximum under cw operation is 730 μW and occurs at a dc current of 76 mA followed by thermal rollover due to Joule heating. The maximum EQE under cw operation is reached at 2.4×10^{-1}% at a dc current of 36 mA. Under pulsed mode operation the thermal effects are greatly reduced and rollover is observed at a current of 500 mA achieving 4.6 mW in output power. The EQE maximum under pulsed mode operation is as high as 3.3×10^{-1}% achieved at a current of 100 mA. With decreasing wavelength the maximum emission power under pulsed mode operation is 1.2 mW, 320 μW, and 19 μW for 232 nm, 228 nm, and 222 nm emission, respectively. The shortest wavelength LED with a peak emission of 217 nm showed a maximum emission power of 3.6 μW at 135 mA under pulsed mode operation. Even though these power levels are relatively modest, the light output is already sufficient to enable applications in the area of gas sensing, e.g. ammonia or nitrogen oxide.[1,2] The corresponding maximum EQEs are decreasing from 9.6×10^{-2}%, 2.7×10^{-2}%, 2.0×10^{-3}%, and 4.9×10^{-4}% for 232 nm, 228 nm, 222 nm, and 217 nm emission, respectively. This trend is in good agreement to recent literature values as shown in Fig. 4.[6–11,20]

In conclusion, we investigated the emission characteristics and operation voltages of deep UV LEDs with emission wavelengths between 239 and 217 nm. When increasing the aluminum composition of the $Al_xGa_{1-x}N/Al_yGa_{1-y}N$ MQW active region, i.e. decreasing the emission wavelength, a strong reduction in light output and EQE is observed. Our findings indicate that this behavior is most likely originating in a decreasing CIE. Additionally, the influence of absorption of the underlying $Al_xGa_{1-x}N$:Si current spreading layer on the spectral characteristics was investigated. By increasing the aluminum composition up to $x = 0.95$, full transparency was maintained for emission >222 nm thus leading to high EQE, however, at the cost of strongly increasing the operation voltage. LEDs emitting at 217 nm grown on $Al_{0.95}Ga_{0.05}N$:Si with on-wafer measured quantum well emission powers of 0.15 μW at 20 mA and 20.1 V were demonstrated in cw operation. Additionally, 239 nm LEDs grown on $Al_{0.90}Ga_{0.10}N$:Si with a maximum integrated output power of 4.6 mW at 500 mA in pulsed mode operation were presented.

Acknowledgments The authors would like to thank Sylvia Hagedorn (Ferdinand-Braun-Institut, Berlin) for providing ELO AlN/sapphire templates, Neysha Lobo-Ploch (UV Photonics NT GmbH, Berlin) for careful proof reading and helpful discussion, and Praphat Sonka (Technische Universität Berlin) for technical support and sapphire polishing. This work was partially supported by the German Federal Ministry of Education and Research (BMBF) within the "Advanced UV for Life" project and by the Deutsche Forschungsgemeinschaft (DFG) within the Collaborative Research Center "Semiconductor Nanophotonics" (SFB 787).

ORCID iDs Frank Mehnke https://orcid.org/0000-0001-5406-0832

1) M. Kneissl and J. Rass, *III-Nitride Ultraviolet Emitters—Technology and Applications* Springer Series in Material Science (Spinger, Cham, 2016) Vol. 227.
2) F. Mehnke et al., IEEE J. Sel. Top. Quantum Electron. **23**, 2000108 (2017).
3) M. Kneissl et al., Semicond. Sci. Technol. **26**, 014036 (2011).
4) R. France, T. Xu, P. Chen, R. Chandrasekaran, and T. D. Moustakas, Appl. Phys. Lett. **90**, 062115 (2007).
5) F. Mehnke, X. T. Trinh, H. Pingel, T. Wernicke, E. Janzén, N. T. Son, and M. Kneissl, J. Appl. Phys. **120**, 145702 (2016).
6) Y. Taniyasu and M. Kasu, Appl. Phys. Lett. **96**, 221110 (2010).
7) H. Hirayama, S. Fujikawa, N. Noguchi, J. Norimatsu, T. Takano, K. Tsubaki, and N. Kamata, Phys. Status Solidi A **206**, 1176 (2009).
8) D. Liu et al., Appl. Phys. Lett. **113**, 011111 (2018).
9) D. Liu et al., Appl. Phys. Lett. **112**, 081101 (2018).
10) C. G. Moe, S. Sugiyama, J. Kasai, J. R. Gradusky, and L. J. Schowalter, Phys. Status Solidi A **215**, 1700660 (2017).
11) F. Mehnke et al., Appl. Phys. Lett. **105**, 051113 (2014).
12) R. G. Banal, M. Funato, and Y. Kawakami, Phys. Rev. B **79**, 121308(R) (2009).
13) C. Reich et al., Appl. Phys. Lett. **107**, 142101 (2015).
14) A. Knauer, A. Mogilatenko, S. Hagedorn, J. Enslin, T. Wernicke, M. Kneissl, and M. Weyers, Phys. Status Solidi B **253**, 1228 (2016).
15) G. Kusch et al., Appl. Phys. Lett. **107**, 072103 (2015).
16) G. Kusch, F. Mehnke, J. Enslin, P. R. Edwards, T. Wernicke, M. Kneissl, and R. W. Martin, Semicond. Sci. Technol. **32**, 035020 (2017).
17) S. P. Grabowski, M. Schneider, H. Nienhaus, W. Mönch, R. Dimitrov, O. Ambacher, and M. Stutzmann, Appl. Phys. Lett. **78**, 2503 (2001).
18) K. Ban, J. Yamamoto, K. Takeda, K. Ide, M. Iwaya, T. Takeuchi, S. Kamiyama, I. Akasaki, and H. Amano, Appl. Phys. Express **4**, 052101 (2011).
19) T. A. Henry, A. Armstrong, A. A. Allerman, and M. H. Crawford, Appl. Phys. Lett. **100**, 043509 (2012).
20) H. Hirayama, Y. Tsukada, T. Maeda, and N. Kamata, Appl. Phys. Express **3**, 031002 (2010).